Journal of the European Ceramic Society **13** (1994) 379–386

Mechanical Properties and Oxidation Behaviour of HIPed Hafnium Nitride Ceramics

M. Desmaison-Brut, J. Montintin

Laboratoire de Matériaux Céramiques et Traitements de Surface, UA CNRS 320, Equipe Ceramiques Nouvelles, 123 Avenue Albert Thomas, 87060 Limoges Cedex, France

F. Valin & M. Boncoeur

CEA, Saclay, 91191, Gif-sur-Yvette Cedex, France

(Received 5 July 1993; revised version received 15 October 1993; accepted 26 November 1993)

Abstract

The compaction at 1600°C, under an isostatic argon pressure of 195 MPa, of a coarse hafnium nitride powder, previously encapsulated in a vacuumed titanium can, has led to the formation of a porous material ($d_r \cong 85\%$).

In order to produce a high-performance material, the same HfN powder has been encapsulated into a silica container and hot isostatically pressed at 1950°C, under a pressure of 195 MPa. In both cases, the dwell time lasted 1 h. Under these conditions, the dense material ($d_r > 95\%$) had a Vickers microhardness H_v^{10N} of 1450, a modulus of rupture rather low (350 MPa) and a SENB fracture toughness of 4·5 MPa $\sqrt{m}$.

The oxidation behaviour, in dry oxygen, suggested that the reaction, between 755 and 950°C, was governed by an interfacial process occurring at the nitride–oxide interface, similarly to the behaviours of dense HIPed TaN and ZrN materials.

Das Pressen eines grobkörnigen Hafniumnitridpulvers, eingeschlossen in eine evakuierte Titanform, ergab bei 1600°C und einem isostatischen Argondruck von 195 MPa ein poröses Material ($d_r \approx = 85\%$).

Um ein besseres Material herzustellen, wurde das gleiche HfN-Pulver in eine Quarzform eingeschlossen und heißisostatisch bei 1950°C und einem Druck von 195 MPa gepreßt. In beiden Fällen betrug die Preßzeit 1 h. Bei diesen Bedingungen besaß das dichte Material ($d_r > 95\%$) eine Vickers-Mikrohärte H_v^{10N} von 1450, einen ziemlich niedrigen Bruchwert (350 MPa) und eine SENB Bruchduktilität von 4·5 MPa $\sqrt{m}$.

Aus dem Oxidationsverhalten in trockenem Sauerstoff läßt sich schließen, daß die Reaktion zwischen 755 und 950°C durch einen Grenzflächenprozeß an der Grenzfläche Nitrid–Oxid bestimmt wurde. Dies entspricht dem Verhalten von dichtem geHIPtem TaN und ZrN.

Le frittage par compression isostatique à chaud (CIC) durant une heure à 1600°C et 195 MPa, d'une poudre commerciale de nitrure de Hafnium précompactée à froid, puis encapsulée dans un container en titane qui est dégazé et scellé, conduit à la formation d'un matériau poreux ($d_r \cong 85\%$).

Le même précompact a été encapsulé dans une ampoule de silice et traité à 1950°C sous une pression de 195 MPa pendant 1 h. Le matériau dense obtenu ($d_r > 95\%$) a une microdureté H_v^{10N} de 1450, un module de rupture assez bas (350 MPa) et une ténacité (SENB) de 4·5 MPa $\sqrt{m}$.

L'étude du comportement à l'oxydation, en présence d'oxygène, de ce dernier matériau suggère que la réaction, entre 755 et 950°C, est régie par un processus interfacial, intervenant à l'interface nitrure–oxyde. Un comportement identique a été observé lors de l'oxydation des nitrures denses TaN et ZrN obtenus par CIC.

Introduction

Hafnium is always found associated with zirconium in the ores. Consequently, commercially available hafnium nitride is not of high purity and contains approximately 2·4% of zirconium. The basic properties of HfN have been summarized in a survey.[1–3] Hafnium nitride has a rather good hardness, but measurements have been mainly done on PVD or CVD coatings. In fact, HfN deposited by CVD represents a promising hard coating for high-speed tools.[3]

Journal of the European Ceramic Society 0955-2219/94/$7.00

HfN thin films, covering the entire composition range from pure Hf to overstoichiometric HfN have been also prepared by reactive magnetron sputtering.[4] On the other hand, at room temperature, the microhardness of PVD coatings was significantly higher than that of the CVD counterparts.[5] Microhardness and electrical resistivity were measured and both properties increased with increasing amount of nitrogen added to the α-Hf phase. For the cubic HfN phase, the Vickers hardness had a maximum of 3500 and the resistivity a minimum of 225 $\mu\Omega$ cm at a composition close to stoichiometry. However, due to intrinsic stresses in the film, both values were considerably higher than those reported for bulk samples (H_v^{50} 1600–2000).

As hafnium nitride is gold-colored, hard coatings for decorative applications were deposited in particular using the cathodic arc process.[6]

Concerning the densification of HfN powder by sintering, few data were reported in the literature.

The hot pressing of transition metal nitrides has been done at different temperatures ranging from 2160 to 2600°C and under various pressures (35 and 45 MPa). The optimization of the working conditions permits the preparation of materials with close-theoretical density.[7] Crucibles were also produced from HfN powder by pressure sintering up to 2200°C, with 96% theoretical density and could be used for stainless steel melts.[8]

The behaviour and properties of this refractory nitride have been studied for aerospace applications but as a tungsten-cermet. Hot pressing has appeared to be satisfactory in fabricating HfN-W cermets for high temperature bearings and for lithium-cooled reactors.[9]

It has been shown that the oxidation of 135 μm thick HfN plates in oxygen, at pressures of 18·7–979 kPa, in the temperature range 730–890°C is governed by an interfacial reaction due to the formation of a non-protective oxide scale consisting of monoclinic hafnia. The oxidation in carbon dioxide between 800 and 1000°C was characterized by an important reduction in the reaction rate and the formation of an intermediate oxynitride phase but the overall kinetic behaviour was identical.[10,11]

The aim of this study was to define precisely the sintering conditions leading to the elaboration of a dense monolithic material and to investigate its mechanical properties and oxidation resistance. The influence of temperature and pressure on the densification is discussed and relationships between the properties and the microstructure are established.

Experimental Procedure

Powder characteristics

H. C. Starck was the supplier of the HfN powder which contains 2·4 wt% of zirconium and other impurities (Table 1). The particle size distribution is bimodal (2–10 μm and 30–50 μm): a significant amount of the powder consisted of large irregular and dense grains which, due to their acicular shape, are still present after sieving at 50 μm.

This powder is slightly substoichiometric as the lattice parameter, obtained by X-ray diffraction analysis, is 4·5204 ± 0·001 Å (lattice parameter of $HfN_{1.005}$: 4·5160 ± 0·0007 Å). If we consider the evolution of the cell parameter with nitrogen vacancies[1] and zirconium impurity,[12] the powder composition may be written $Hf_{0.951}Zr_{0.049}N_{0.941}$.

Process

The hafnium nitride powder was cold isostatically pressed at 250 MPa and the green moulded material was introduced either into a silica or a titanium container. An inert BN layer, which acted as a diffusion barrier, was necessary to prevent chemical reactions between the capsule and the component. Degassing was carried out at 600°C in vacuum for 12 h. The HIP parameters (temperature and pressure) were defined by taking into consideration the plastic deformation of the container. The ceramic material was sintered either at 1600–1630°C (Ti container) or up to 1950°C (silica can). The maximum pressure applied for 1 h dwell time was 195 MPa.

Specimen characterization

The density measurements were done using the Archimedes method on 20 cubic samples (4 × 4 × 4 mm^3). The microstructure was characterized by scanning electron microscopy (SEM) observations on chemically etched samples (etching medium HF/HNO_3). Microhardness tests were carried out using a selected load of 1 kg. The single edge notched beam (SENB) method was used to determine the critical stress intensity (K_{1c}) factor, on a minimum of four samples. A total of 5–7 4/4/22 mm^3 bars were tested for three-point bending strength measurements (load application speed 0·2 mm mn^{-1}, span distance 19 mm). Thermal quenching was performed by heating specimen bars (4/4/22 mm^3), dropping them into a room-temperature water bath and then measuring fracture strength.

Table 1. Chemical analysis of starting powders (wt%)

Hf + Zr	Zr	N	O	C	Fe	Al
92·69	2·4	7·02	0·489	0·22	0·025	0·07

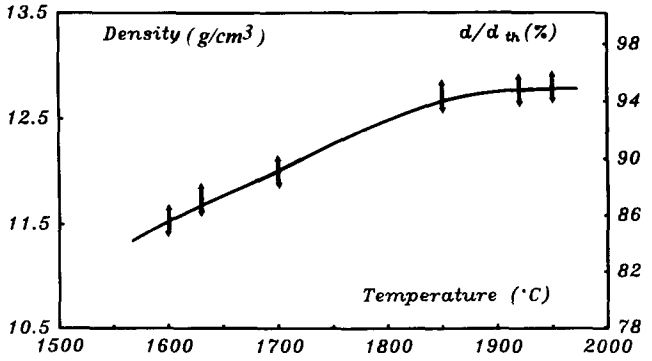

Fig. 1. Influence of the applied sintering temperature on densification, 1 h dwell time (195 MPa).

The Young's modulus (E) was determined at room temperature by the disc vibration technique. The oxidation resistance was tested in a dynamic flow of pure oxygen (20 litres/h) at atmospheric pressure in a Setaram thermobalance. The kinetic curves were obtained by plotting the fractional weight change $\alpha(\alpha = \Delta m/\Delta m_\infty)$ versus time. The weight gain Δm_∞ corresponds to the complete oxidation evaluated by considering that HfN is transformed into HfO_2 according to the reaction:

$$2HfN + 2O_2 \rightarrow HfO_2 + N_2 \qquad (1)$$

Results and Discussion

Densification and mechanical properties

In all cases, the HIP treatment did not induce a change in the stoichiometry of materials. The influence of applied temperature on densification is shown in Fig. 1.

Treatment in a titanium capsule at 1600°C, 195 MPa, for 1 h dwell time permitted a relative density, d_r, of 85% to be achieved. From 1700°C to 1950°C, by using silica containers, the density increased to a maximum of 12·96 g/cm³ (>95%).

The elimination of the residual porosity was difficult to obtain. This is mainly due to the high melting temperature of HfN which is much greater than those of titanium, tantalum or zirconium nitrides whose HIPing has been previously

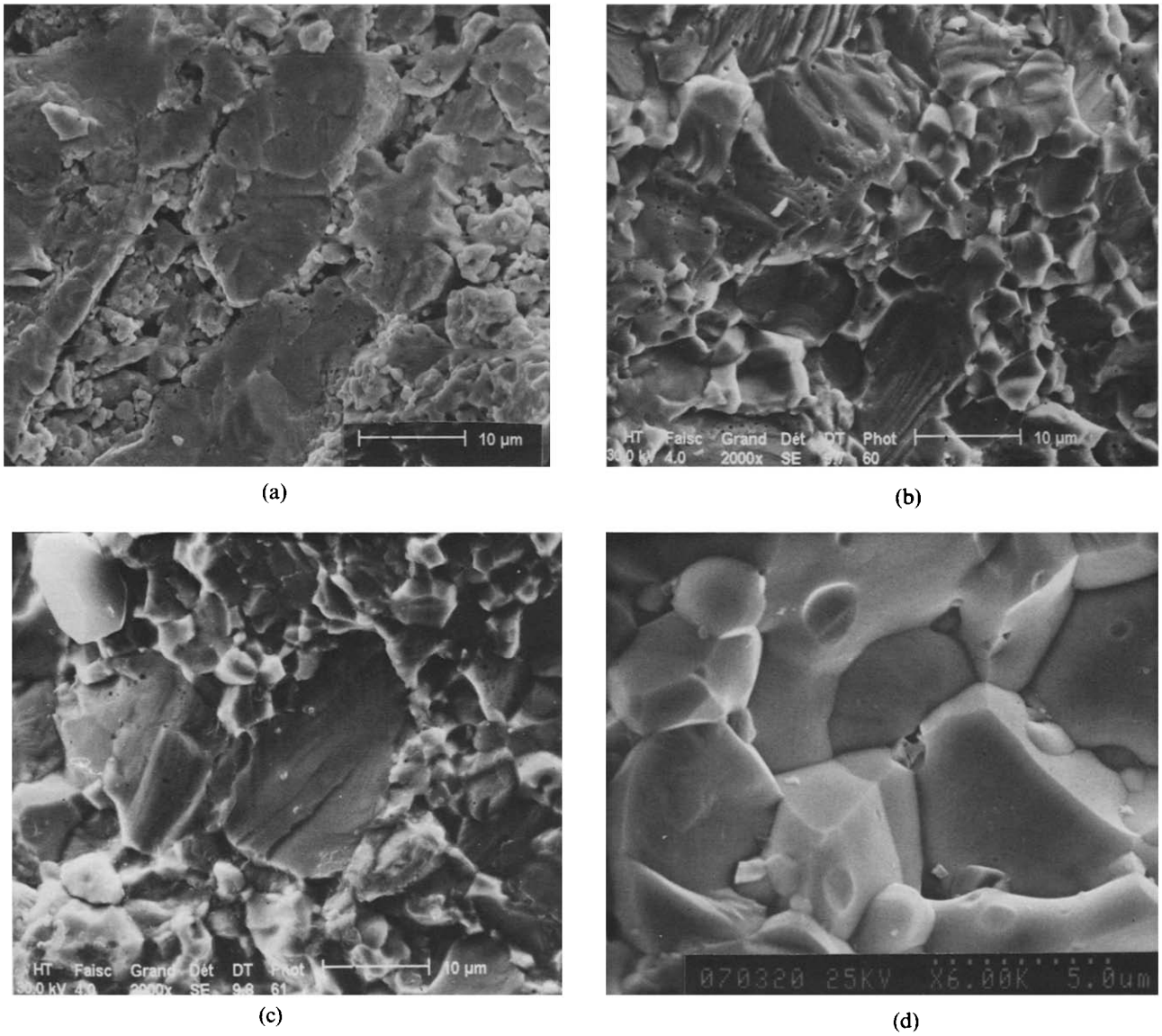

Fig. 2. Scanning electron micrographs of fracture surfaces; (a) 1600°C; (b) 1850°C; (c) 1950°C; (d) 1950°C.

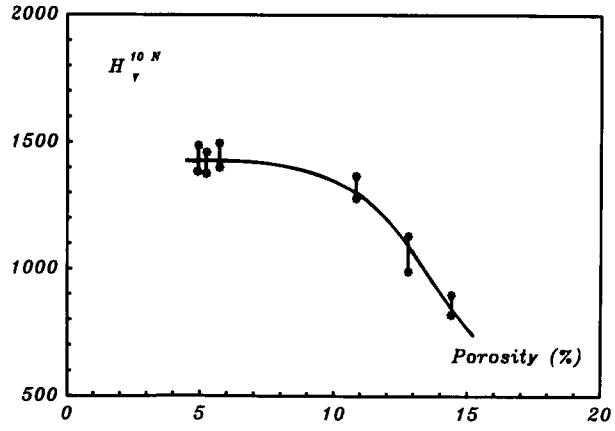

Fig. 3. Evolution of Vickers microhardness with porosity.

studied.[13–15] The impossibility of reaching complete densification was also linked to powder characteristics: an irregular grain shape and a large size distribution of particles used to enhance the sintering process. Small isolated porosities were still observed in the core of the largest grains and were difficult to eliminate. The origin of the heterogeneity of the microstructure is obvious. Indeed, the coalescence of the small particles with the large grains was difficult to obtain and consequently the densification was incomplete. At the highest temperatures, a line of small porosities was located at the periphery of the biggest grains (Fig. 2).

Three stages of sintering have been identified for the hot pressing of transition metal nitride.[7] In the first stage of the densification, particle sliding takes place, followed by dislocation redistribution. Sliding annihilation in the second stage leads to polygonalization and formation of grains and subgrain boundaries. Finally, in the third stage, diffusional viscous flow occurs in relation to small particle coalescence.

In the case of HfN, it was shown by Petrykina and Shvedova[7] that the controlling mechanism of the densification was the viscous flow independently of pressure. The present results are in agreement with this model as confirmed by micrographs showing that grain growth essentially has occurred on the smallest grains (Fig. 2).

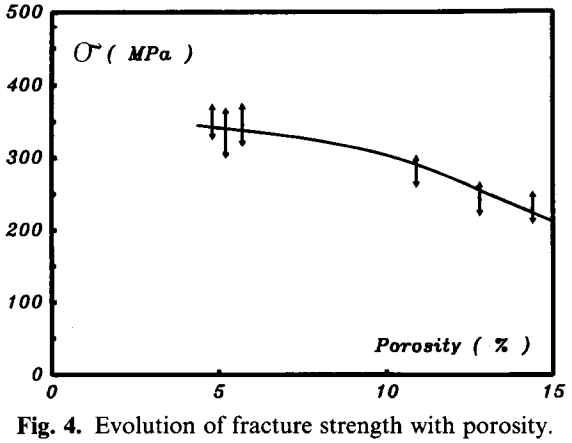

Fig. 4. Evolution of fracture strength with porosity.

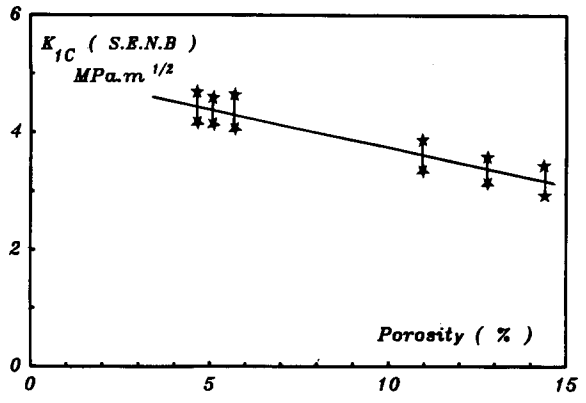

Fig. 5. Influence of porosity on fracture toughness.

The Vickers microhardness followed a classical law and increased with densification (Fig. 3). Compared with the H_v^{10N} value of HfN coatings (greater than 2000 Vickers), the maximum value obtained on the densest material was much lower (H_v^{10N} = 1450). This value was a constant for the three densest materials: in fact, as the difference in porosity was less than 2% and as the pores were mainly located inside the biggest grains, the hardness difference was not tangible. The same correlations will be noticed for flexural strength and fracture toughness values.

The statistical variation in strength (σ_f) at room temperature is shown as a function of porosity in Fig. 4. The maximum value obtained was 354 MPa with a standard deviation of 19 MPa. The best fitted equation based on experimental values led to a maximum value of 361 ± 20 MPa for a material of zero porosity and is lower than the only value available in literature (σ_f = 475 ± 25 MPa), concerned with a cermet (90% HfN–10% W).[9]

In a general way, the modulus of rupture σ_f decreases linearly or exponentially as porosity increases, but σ_f also depends on the grain size according to the relation:

$$\sigma_f = Ad^{-1/2} \qquad (2)$$

where A is a constant and d is the grain diameter.

In the present work, as the porosity decreases, the small particles coalesce and the average grain size increases. This could partially explain the constant properties of the three densest grades as suggested above for the microhardness.

The evolution of fracture toughness was similar to the evolution of the modulus of rupture (Fig. 5)

Table 2. Results of fitting data to different equations (E and E_0 are respectively the Young's moduli of the porous and non-porous materials, a is an empirical constant and P the volume fraction porosity)

	$E = E_0(1 - aP)$	$E = E_0[\exp - aP]$	$E = E_0\left(\frac{1-P}{1+aP}\right)$	$E = E_0[1 - aP^{2/3}]$
E	512±12 GPa	556±5 GPa	611±6 GPa	587±20 GPa
a	3·46±0·25	5·30±0·50	7·11±0·20	2·04±0·51

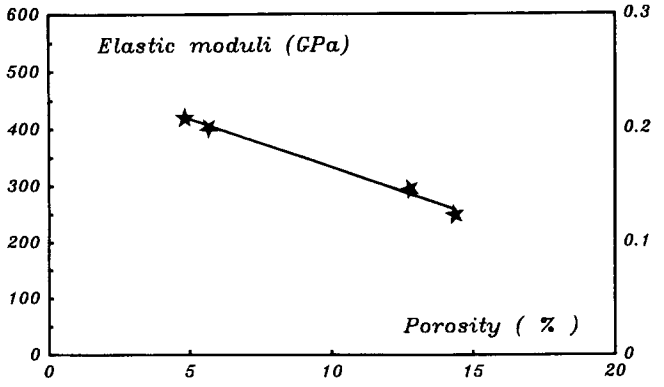

Fig. 6. Elastic parameter E versus porosity curves.

and the maximum value was 4·5 ± 0·3 MPa$\sqrt{m}$. By applying a linear law, the extrapolation at zero porosity gave a value close to 5 MPa$\sqrt{m}$, identical to the toughness value of a dense HIP titanium nitride material, but lower than ZrN (6 MPa$\sqrt{m}$) or TaN (7 MPa$\sqrt{m}$) K_{1c} values.[13–15]

From the modulus of rupture and the fracture toughness values, the largest defect size may be calculated by the relation:

$$a_c = \frac{(K_{1c})^2}{\pi\, 1{\cdot}21\, \sigma_f^2} \qquad (3)$$

The corresponding critical flaw size value of 44 μm is of the order of the size of the biggest grain and much greater than the pore size. However, agglomerations of small particles which induced a concentration of voids and created porosity areas might have caused the rupture.

The fracture surfaces of samples sintered at different temperatures are presented in Fig. 2. The rupture was intergranular in the small grain size regions but transgranular for large grains. For samples treated at temperatures ranging from 1900°C to 1950°C, small spherical grains were regularly distributed along the grain boundaries.

Elastic properties

For oxide materials, many equations have been proposed to relate the porosity to the elastic modulus E.[16] These equations, applied to our data, gave by extrapolation at zero porosity, the elastic constant values of a dense HfN material (Table 2). The insufficient number of experimental data did not permit a conclusion about the best fitted relation (Fig. 6). Actually, the literature data concerning HfN elastic parameters are very poor. Bogdanov *et al.*[17] have estimated the elastic modulus of group III–V transition metals and proposed an elastic modulus value of 480 GPa for an $HfN_{1\cdot01}$ material.

The thermal shock resistance, σ_f, is an important property especially for high temperature applications. Quenching experiments have clearly shown unstable crack propagation. The experimentally determined critical temperature difference ΔT_c after water quenching, for the two grades was slightly dependent (207 and 213 K), on porosities (5 and 13%) (Fig. 7). The higher the porosity, the higher the ΔT_c value, which was not expected. This result has already been observed in the case of HIPed TiN materials having a small porosity differences (ΔT_c = 207 K, TiN porosity = 0·75% and ΔT_c = 223 K, TiN porosity = 3%).[13]

Thermal shock resistance, like elastic properties, is generally affected by microstructure, in particular pore characteristics, i.e. size, location, shape. . . . High density values generally improve the thermal shock resistance. In fact, the influence of pore size on thermal shock resistance to fracture initiation is defined by the increase in flaw size when the pore size increases. Here, it is necessary to analyse the influence of each microstructural characteristic on σ_f and ΔT_c. As the density increases, voids, which were located along the grain boundaries, progressively disappeared and only small spherical porosities were retained, mainly inside the biggest grains. Also, there was an increase in the smallest grains by coalescence but no real growth of the biggest ones.

Oxidation

The oxidation in dry oxygen of the dense HfN grade (characterized by closed porosity) started approximately at 800°C and the reaction accelerated above 1000°C (Fig. 8). The shape of the isothermal curves, recorded at atmospheric pressure, was linear at low temperatures (750–800°C) but showed some deceleration in the upper tempera-

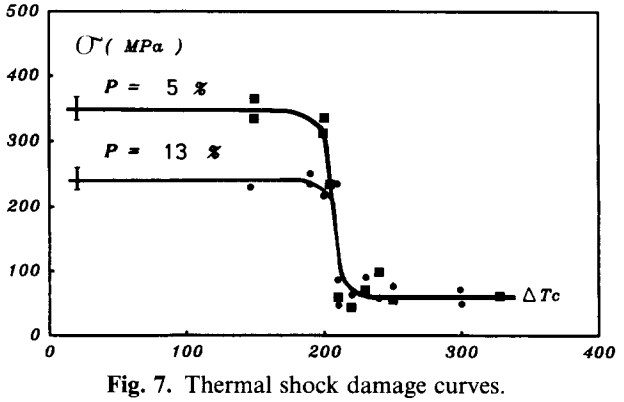

Fig. 7. Thermal shock damage curves.

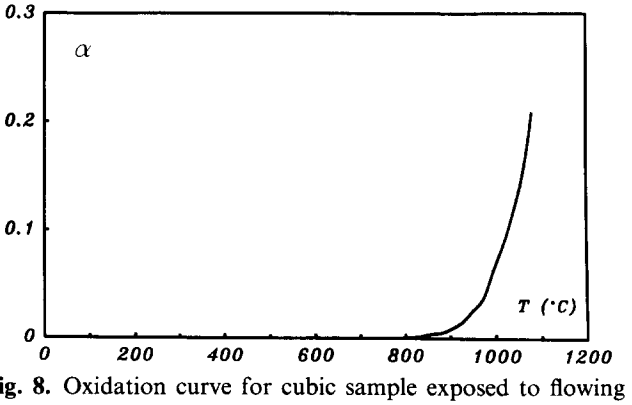

Fig. 8. Oxidation curve for cubic sample exposed to flowing oxygen at 100 kPa,

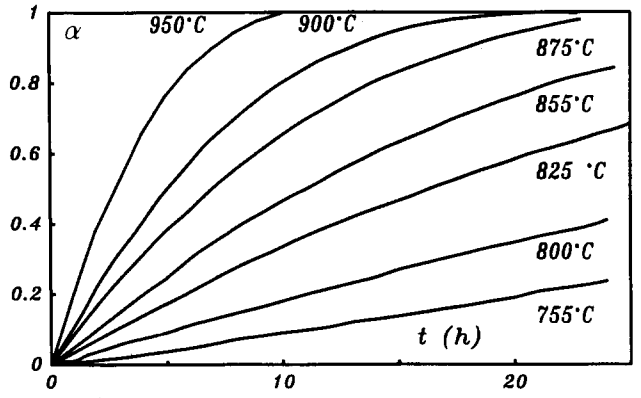

Fig. 9. Isothermal kinetics recorded at 1 atm in the temperature range 755–950°C.

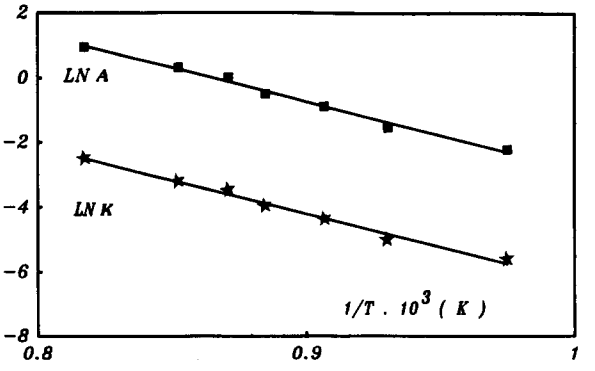

Fig. 11. Influence of temperature on the rate constant K and on the affinity at 1 atm.

ture range (825–950°C). The specimen was totally oxidized after 20 h at 900°C (Fig. 9).

The kinetic behaviour is similar to those of HIPed dense zirconium nitride and tantalum nitride materials previously studied in an oxygen atmosphere.[13–15] Each isothermal curve could be superimposed onto any other by an affinity relationship with time (Fig. 10). A master run roughly in the middle of the series was chosen and a factor A was calculated for each curve such that multiplication of the time scale of the run by A would superimpose onto the master run curve. Log A was found to be a linear function of $1/T$ (Fig. 11). This implies that the activation energy is unique over the whole temperature range: $E = 173 \pm 10$ kJ/mole.

To assess the effective contribution of the oxygen partial pressure on the reaction rate, isobaric kinetics were recorded at 835°C, in the pressure range 20–100 kPa and plotted as a function of time (Fig. 12). The general shape of the kinetics is maintained and the curves can be superimposed. As both isothermal and isobaric curves are in a close affinity relationship with time, the equation can be written as a function of separated variables:

$$v = \frac{d\alpha}{dt} = f(\alpha)g(T)h(P) = \text{Constant}\, f(\alpha)h(P) \exp \frac{E}{RT} \quad (4)$$

where $f(\alpha)$ is a morphological term characteristic of the reaction area. This means that the controlling process is unique over the whole reaction range.

Monoclinic hafnia is formed independently of pressure and temperature but the morphological aspect of the oxide is different with temperature: the powdered oxide which is formed at low temperature sinters as the temperature increases, leading to the formation of a Maltese cross (Fig. 13).

The low plasticity of the oxide formed at a lower temperature than the Tammann temperature ($\cong 0{\cdot}5\ T_f$), $T = 1450$°C, does not allow the stresses to relax and provokes the opening of the cube edges; indeed, the value of the Pilling–Bedworth ratio, $\Delta = 1{\cdot}42$ (volume expansion coefficient) is inducing the formation of compressive stresses in the scale. Morphological parameters such as the formation of a lamellar and porous oxide and the opening of the cube edges, clearly demonstrate that the oxidation is not governed by a diffusion process. Previous studies have shown that the oxidation behaviour in oxygen of 135 μm thick $HfN_{0{\cdot}93}$ plates was governed by reaction (1) located at the nitride–oxide phase boundary, due to the formation of non-protective HfO_2 simultaneously with cracks in the core.[10]

The internal attack of the substrate by means of an intergranular cracking process equivalent to a branched chain germination, explained the sigmoidal shape of the kinetics. Here, such

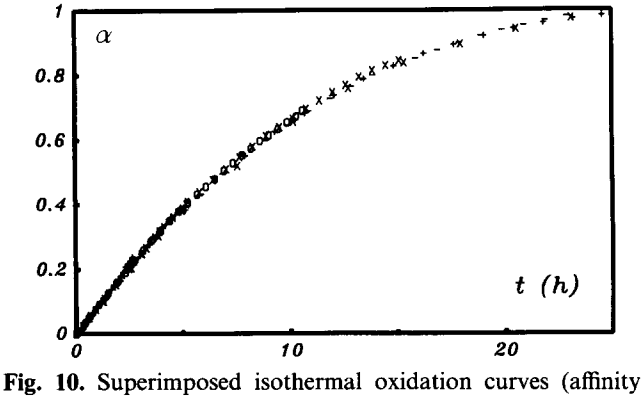

Fig. 10. Superimposed isothermal oxidation curves (affinity versus time).

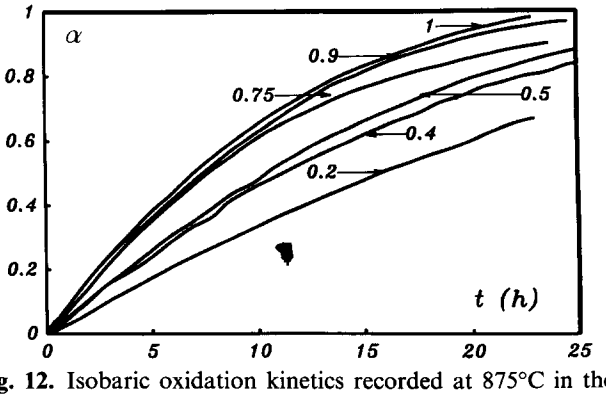

Fig. 12. Isobaric oxidation kinetics recorded at 875°C in the pressure range 20–100 kPa (0·2–1 atm).

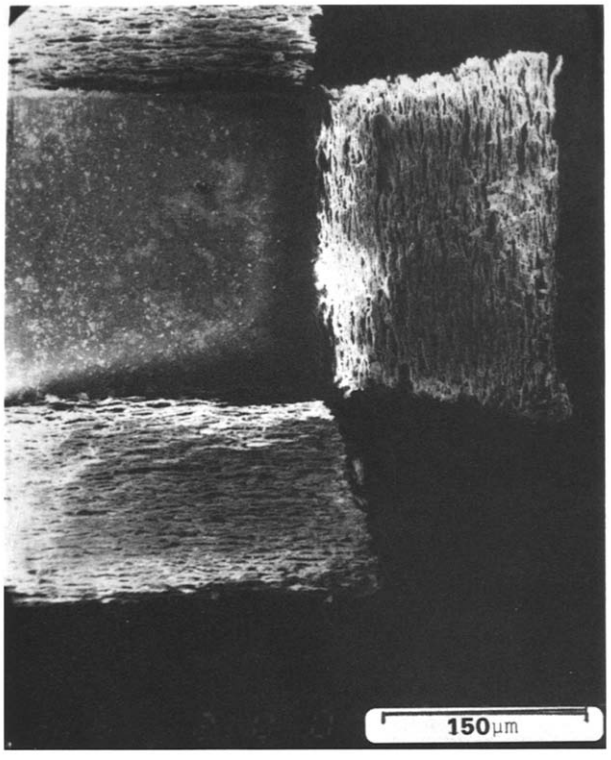

Fig. 13. The oxide scale Maltese cross obtained at 875°C after 15 h oxidation (P = 100 kPa).

internal oxidation of the nitride was not observed. Therefore, the rate, v, should be directly proportional to the surface area, S, of the non-oxidized cubic nitride core of edge, a, at time t. A detailed description of this oxidation mechanism, recently presented in a paper devoted to the reactivity in oxygen of HIPed zirconium nitride,[18] has shown that:

—The reactive surface and by extension the reaction rate are related to the conversion degree α through:

$$v = \frac{d\alpha}{dt} = k_{(T,P)}S(\alpha) \quad (5)$$

$$S(\alpha) = f(\alpha) = 3(1 - \alpha)^{2/3} \quad (6)$$

—the integration of expression (5) leads to:

$$F(\alpha) = 1 - (1 - \alpha)^{1/3} = K_{(T,P)}t \quad (7)$$

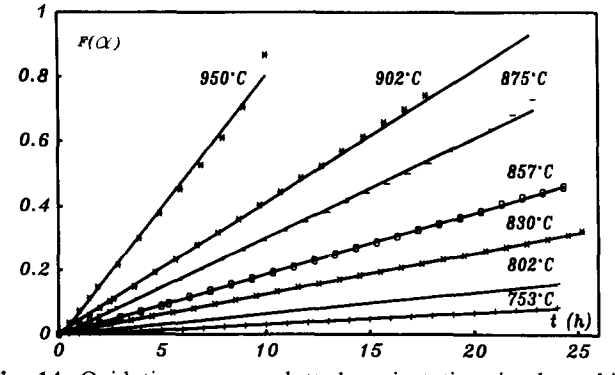

Fig. 14. Oxidation curves plotted against time in the cubic form at various temperatures.

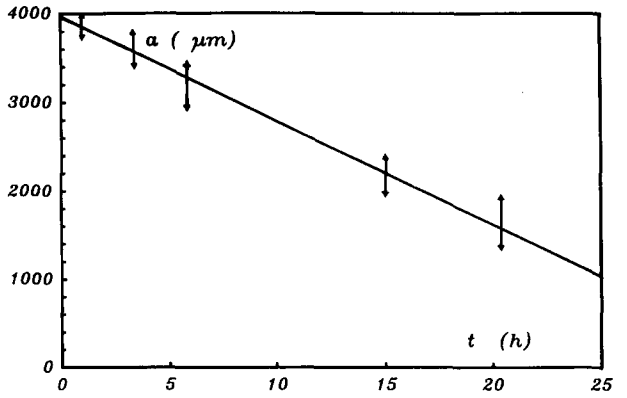

Fig. 15. Time dependence of hafnium nitride core edge a at 875°C.

—the edge a of the non-oxidized cubic core decreases linearly:

$$a = a_0 - K'_{(T,P)}t \quad a_0 \text{ being the initial edge} \quad (8)$$

$F(\alpha)$ versus t has been plotted in Fig. 14. As can be seen, linear plots are obtained for all temperatures up to 950°C. At 875°C, the core edge, a, has been measured as a function of time (Fig. 15). A linear dependence is observed in accordance with eqn (8).

By plotting ln K versus reciprocal temperature (Fig. 11), a value of 175 ± 8 kJ/mol is obtained, this value being identical to the preceding one derived from the log $A = f(1/T)$ plot. The constant K is also influenced by a change in oxygen pressure, P. The constant dependence with pressure may be represented by a Langmuir type homographic relationship:

$$K = aP/(1 + bP) \quad (9)$$

where a = 9·77 and b = 1·97 (Fig. 16).

Finally, the kinetic law may be represented by the following equation:

$$V = \text{Constant}\ (1 - a)^{2/3} \cdot 9{\cdot}77P/(1 + 1{\cdot}97P) \exp - 174/RT \quad (10)$$

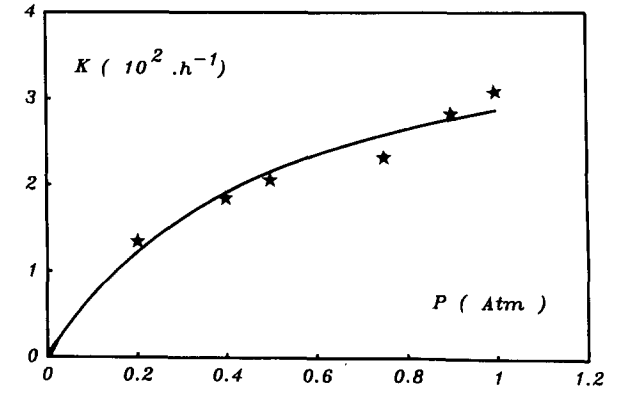

Fig. 16. Effect of oxygen pressure on the rate constant K at 875°C.

Conclusion

Hafnium nitride is a highly refractory nitride. As a consequence, the full densification of a coarse hafnium nitride powder is difficult to obtain. At high temperatures (1950°C) and high pressures (195 MPa), for 1 h dwell time, a minimum porosity (4%) still remains. Pores are mainly located inside the biggest grains (core and periphery).

For temperatures ranging from 1850 to 1950°C, we have observed a small density increase and consequently a minor difference between the mechanical properties of the three densest materials. On the other hand, comparing two different grades with 5 and 13% porosities, no tangible difference in the thermal shock resistance was observed. This was due to the microstructure evolution as grain coalescence has occurred simultaneously with porosity decrease.

If we compare the oxidation behaviour of HIPed transition metal nitrides as ZrN (d_r > 98%), HfN (d_r > 95%) or TaN (d_r > 99%), the hafnium nitride material which contains at least 4% of internal pores, is the most resistant. Nevertheless, the three studies have shown the formation of a non-protective scale, the reacting gas (O_2) rapidly reaching the substrate and the nitrogen gas easily diffusing outwards; consequently the oxidation of cubic specimens was governed by an interfacial type process located at the nitride–oxide interface.

We may conclude that the mechanical and oxidation behaviours of the studied materials could be improved by using a finer and more homogeneous grain size powder which should lead, without an increase in the temperature process, to a totally dense ceramic.

References

1. Perry, A., Refractories HfC and HfN—a survey: I, Basic properties. *Powder Metall. Int.*, **19**(1) (1987) 29–35.
2. Perry, A., Refractories HfC and HfN—a survey: II, Phase relationships. *Powder Metall. Int.*, **19**(2) (1987) 32–6.
3. Perry, A., Refractories HfC and HfN—a survey: III, Cemented carbides and coatings. *Powder Metall. Int.*, **19**(6) (1987) 17–19.
4. Johansson, B. O., Sundgren, J. E. & Helmersson, U., Reactive magnetron sputtered hafnium–nitrogen films. II Hardness and electrical resistivity. *J. Appl. Phys.*, **58** (1985) 3112–17.
5. Quinto, D. T., Wolfe, G. J. & Jindal, P. C., High temperature microhardness of hard coatings produced by physical and chemical vapor deposition. *Thin Solid Films*, **153** (1987) 19–36.
6. Randhawa, H., Hard coatings for decorative applications. *Surf. Coat. Technol.*, **36** (1988) 829–36.
7. Petrykina, R. Y. & Shvedova, L. K., Hot pressing of transition metal nitrides and their properties. *Poroshk., Metall.*, **12** (1972) 27–31.
8. Schumacher, G., Rolf, H. & Heinzel, V., New pressure sintering methods for extreme temperatures. *LaborPraxis*, **4**(3) (1980) 16–18.
9. Gangler, J. J., Nasa research on refractory compounds. *High Temp.-High Press.*, **3**(5) (1971) 487–502.
10. Desmaison, J., Desmaison-Brut, M. & Billy, M., Oxydation du nitrure de hafnium par l'oxygène. *Annal. Chim.*, **4** (1979) 85–92.
11. Desmaison-Brut, M., Desmaison, J. & Billy, M., Oxydation du nitrure de hafnium par le dioxyde de carbone, *Anal. Chem.*, **10** (1985) 93–103.
12. Giorgi, A. L., Szklarz, E. G. & Wallace, T. C., Anomalous superconducting properties of carbides and nitrides of group IVa and Va elements, *J. Brit. Ceram. Soc.*, **10** (1968) 183–93.
13. Desmaison-Brut, M., Themelin, L., Valin, F. & Boncoeur, M., Mechanical properties of HIPed titanium nitride. In *Euro-Ceramics, Vol. 3, Engineering Ceramics*, ed. G. de With, R. A. Terpstra & R. Metselaar. Elsevier Applied Science, London, New York, 1989, pp. 3, 258–62.
14. Montintin, J., Desmaison-Brut, M., Boncoeur, M. & Valin, F., Microstructure, mechanical properties and oxidation behaviour of hot isostatic pressed tantalum nitride. In *Proceedings of hot isostatic pressing: Theory and Applications*, ed. R. J. Schaefer & M. Linzer. American Society of Metals International, Ohio, 1989, pp. 233–8.
15. Alexandre, N., Desmaison-Brut, M., Valin, F. & Boncoeur, M., Mechanical properties of hot isostatically pressed zirconium nitride materials. *J. Mater. Sci.*, **28** (1993) 2385–90.
16. Phani, K. K. & Niyogi, S. K., Young's modulus of porous brittle solids, *J. Mater. Sci.*, **22** (1987) 257–63.
17. Bogdanov, V. S., Neshpor, V. S., Kondrashev, Yu. D., Goncharuck, A. B. & Pityulin, A. N., Relation between temperature and lattice parameter of nitrides of group III–V transition metals. *Poroshk. Metall.*, **5** (1982) 79–84.
18. Alexandre, N. & Desmaison-Brut, M., Reactivity in oxygen of a HIPed zirconium nitride material. *J. Europ. Ceram. Soc.*, **8** (1991) 285–90.